2006

TWO CHEMICAL SPILL PATTERNS IN TIDALLY DOMINATED SAN DIEGO BAY

Chu, Peter C.

Published in Coastal Environment and Water Quality (ed. by Y. J. Xu & V. P. Singh), 69-90.

6

TWO CHEMICAL SPILL PATTERNS IN TIDALLY DOMINATED SAN DIEGO BAY

Peter C. Chu and Kleanthis Kyriakidis
Department of Oceanography, Naval Postgraduate School, Monterey, CA 93943, USA

Steven D. Haeger
Naval Oceanographic Office, Stennis Space Center, MS 39529, USA

Mathew Ward
Applied Science Associates, Inc., 70 Dean Knauss Drive, Narragansett, RI 02882, USA

ABSTRACT

A coupled hydrodynamic-chemical spill model is used to investigate the chemical spill in the San Diego Bay. The hydrodynamic model shows that the San Diego Bay is tidally dominated. The chemical spill model shows the existence of two different patterns of chemical spill for pollution (methanol, benzene, liquefied ammonia, etc.) released at 0.5 m depth in the north (32°43'N, 117°13.05' W) and the south bays (32°39'N, 117°07.92' W). For the north-bay release, the chemical spill in the whole basin with a fast speed of spill in the northern part (12 hours) and a slow speed of spill in the southern part (20 days) with very small concentration. For the south-bay release, the chemical pollutants are kept in the southern part. Very few pollutants reach 32°41'N parallel (the boundary between the north and south bays).

6.1. INTRODUCTION

San Diego Bay (Figure 1) is located near the west coast of southern California. It is a relatively small basin (43-57 km^2) nearly 25 km long and 1-4 km wide. It shapes a flipped Γ-type and extends to the north to the city of San Diego and to the south to Coronado Island and Silver Strand, with a northwest to southeast orientation. It is a natural harbor sheltered by overlapping peninsulas (in west Point Loma and in east Coronado). San Diego, being the last southwest major city neighboring Mexico, is a very important port, especially for the U.S. Navy, since it hosts the headquarters of the 11^{th} U.S. Naval District and a large portion of the American Fleet. The topography is not homogeneous (Figure 2), and the average depth is of 6.5 m (measured from the mean sea level). The northern/outer part of the bay is narrower (1-2 km wide) and deeper (reaching depth of 15 m) and the southern/inner part is wider (2-4 km wide) and shallower (depth less than 5 m). Since San Diego is a semi-closed bay, it exchanges with the Pacific Ocean only through a single channel at the mouth. Near the mouth of the bay, the north-south channel is about 1.2 km

wide, bounded by Point Loma to the west and Zuniga jetty to the east with depths between 7 and 15 m (Chadwick and Largier, 1999a). The western side of the channel is shallower than the east side.

The shoreline landscape of San Diego Bay is spotted with highly polluting shipbuilding and ship repair facilities. Navy and civilian ship operations including recreational boating are other sources of pollution in the San Diego Bay. These toxins threaten public health and the environment. Investigation of the chemical dispersion of floating chemicals such as methanol, benzene and ammonia is very important for the water quality control. Besides, in the current threat environment, a chemical attack in a big city hosting a large portion of the U.S. Naval bases (such as San Diego) is anything but impossible. To evaluate the chemical treat, we first need to identify the chemical spill pattern for floating chemicals (e.g., methanol, benzene and ammonia), sinking chemicals (e.g., chlorobenzene and trichloroethylene) and dispersing chemicals to the air (e.g., naphthalene). In this study, a coupled hydrodynamic-hydrochemical fate model is used to identify the pollutant dispersion patterns. The hydrodynamic sub-model is driven by tides and winds and predicts the velocity field. The hydrochemical model is driven by the velocity field and predicts the chemical spill.

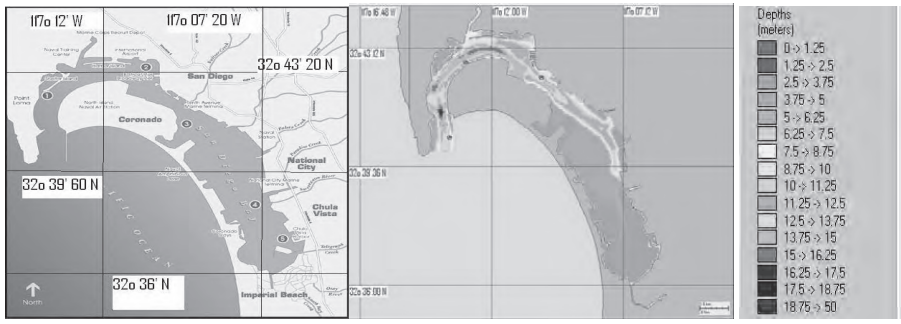

(a) **(b)**

Fig. 1. San Diego Bay (a) main geographical locations in (from: http://sdbay.sdsc.edu/html), and (b) bathymetry.

6.2. BACKGROUND

6.2.1. Tidal Basin

Since San Diego is a semi-closed bay, it exchanges with the Pacific Ocean only through a single channel at the mouth. Near the mouth of the bay, the north-south channel is about 1.2 km wide, bounded by Point Loma to the west and Zuniga jetty to the east with depths between 7 and 15 m (Chadwick and Largier, 1999a). The western side of the channel is shallower than the east side. The topography is not homogeneous (Figure 2), and the average depth is of 6.5 m (measured from the mean sea level). The northern/outer part of the bay is narrower (1-2 km wide) and deeper (reaching depth of 15 m) and the southern/inner part is wider (2-4 km wide) and shallower (depth less than 5 m).

San Diego Bay is a perfect example of a tidal basin connected to the ocean by an inlet with an artificial jetty (Zuniga) built to control beach erosion. The Zuniga jetty extends

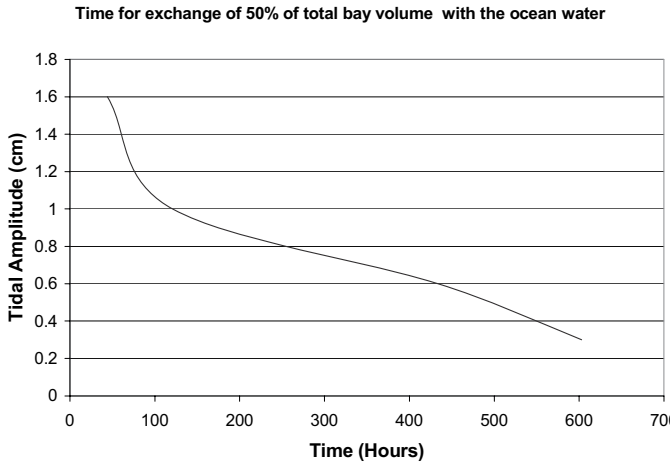

Fig. 2. Time for exchange of 50% of total bay volume with the ocean water (from the website: http://sdbay.sdsc.edu/html/modeling2.html).

almost one mile offshore Zuniga Point and most of it is not clearly visible at high water (Figure 3). Obviously, the bay has been intensively engineered to accommodate shipping activities. Ninety percent of all available marsh lands and fifty percent of all available intertidal lands have been reclaimed and dredging activities within the bay have been equally extensive (Peeling, 1975; Wang et al., 1998). Kelp forests extend approximately 2 km south of Point Loma and along its western side. They are quite thick and they create seasonal dumping of currents to about one-third their values outside (Jackson and Winant, 1983).

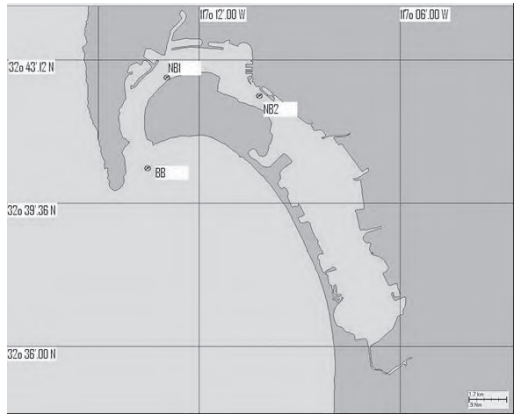

Fig. 3. Location of the ADCP stations deployed by SPAWAR in June to August 1993. Note that Station-bb is at the mouth of the San Diego Bay.

Currents in San Diego Bay are predominately produced by tides (Wang et al., 1998). This tidal exchange between the ocean and the bay is a result of a phenomenon called “tidal pumping” (Fischer et al., 1979). The “pumping” of water is caused due to the flow difference between the ebb and the flood flows.

Being located at mid-latitude, tides and currents within the San Diego Bay are dominated by a mixed diurnal-semidiurnal component (Peeling, 1975). The tidal range from mean lower-level water (MLLW) to mean higher-high water (MHHW) is 1.7 m with extreme tidal ranges close to 3 m (Chadwick and Largier, 1999a). Typical tidal current speeds range between 0.3-0.5 m/s near the inlet and 0.1-0.2 m/s in the southern region of the bay (Wang et al., 1998). The phase propagation suggests that the tides behave almost as standing waves with typical lags between the mouth and the back portion of the bay of 10 min and a slight increase in tidal amplitude in the inner bay compared to the outer bay. The overall tidal prism for the bay is 5.5×10^7 m^3 and the tidal excursion is larger than the mouth with a value of 4.4 km (Chadwick and Largier, 1999b). Offshore the Bay, the average current speed is 0.1 m/s. The currents are equator ward in all seasons and ninety percent of their measurements range between 1 and 0.25 m/s (Jackson and Winant, 1983).

The form ratio (ratio between diurnal -K1+O1- and semidiurnal -M2+S2-) shows that the tidal constituents are mixed (Table 1). Although there are 21 harmonic tidal constituents, it is possible to approach the solution by using four or five (including N2).

Table 1. The mixed diurnal-semidiurnal nature of San Diego Bay tides. (From: National Ocean Service (NOS) accepted harmonic constants for station number 9410170 in San Diego, CA Latitude: 32° 42.8' N Longitude: 117°10.4' W).

	Name	Amplitude (m)	Epoch (degrees)
1	M2	0.576	148.9
2	S2	0.233	145.9
3	N2	0.136	128.7
4	K1	0.352	210.5
5	O1	0223	195.6
6	NU2	0.027	134.3
7	MU2	0.010	109.7
8	2N2	0.018	108.7
9	OO1	0.010	225.4
10	LAM2	0.004	147.5
11	M1	0.011	194.2
12	J1	0.018	217.9
13	SSA	0.017	272.7
14	SA	0.063	182.0
15	RHO	0.008	189.2
16	Q1	0.041	188.7
17	T2	0.014	145.9
18	2Q1	0.006	180.7
19	P1	0.109	208.8
20	L2	0.013	121.7
21	K2	0.065	139.3

Since San Diego Bay has a relatively narrow mouth and a large portion of shallow water, the percentage of total bay water exchanged during a tidal cycle can be quite significant. At mean low low water, the bay has a surface area of 4.3×10^7 m^2 and a volume

of 2.795×10^8 m^3. At the mouth of the bay, the tidal prism, or volumetric flux passing a cross-section during a single flooding cycle, can reach 40% of the mean volume of the bay during a strong flood. For an average tidal cycle, the tidal prism at the mouth is about 13% of the mean total bay volume. During a single tidal cycle, water from the front portion of the bay mixes with open ocean water and exchanges with the bay water that existed on the previous cycle. This open ocean water exchanges further into the bay on successive cycles (Figure 2).

6.2.2. Barotropic Basin

San Diego Bay is a barotropic basin. This can be verified by data from three ADCPs (Figure 3) deployed by SPAWAR in 1993. The first was a broad band one (bb) and was deployed in position (32°42'25.8"N, 117°13'30.6" W) from June 22 until July 23, 1993. The second was a narrowband one (nb1) and was deployed in position (32°42'43.98"N, 117°12'55.68"W) from June 22 until August 26, 1993. The last was a narrowband one (nb2) and was deployed in position (32° 42' 17.22"N, 117°10' 8.88"W) from June 23 until August 27, 1993. By checking the ADCP data inside the bay (nb1, nb2), San Diego Bay was concluded to be vertically well mixed. This can be confirmed from time series of (u, v) components at station-nb2 in three different depths from the ADCP measurements. For nb2, the correlation coefficient between the surface and bottom is 91.89% for the u-component and 94.71% for the v-component 96.32%. Between the surface and bottom, the phase matches very well and so does the trend in the respective amplitudes. In terms of actual amplitude matching, it is possible to optically verify the good match. The differences observed cannot contradict that San Diego Bay is well mixed.

6.2.3. Hydrographic Features

Freshwater inflow to the bay is minimal, comes less from the Otay River and mainly from the Sweetwater River located to the southern part of the Bay and occurs only during winter storms. Both rivers are regulated by storage reservoirs. The San Diego River has been diverted by the U. S. Army Corps of Engineers since 1875 and no longer empties into San Diego Bay.

San Diego Bay can be regarded as a vertically well-mixed estuary (Wang et al., 1998). In the south bay, the currents are much smaller than in the north and the model performance cannot be well documented. The average water temperature in San Diego Bay is 21°C and ranging between 14°C and 26°C. The average temperature during the summer (late June to late August) is 23°C. Using data from five different stations of the Bay Wide Water Quality Monitoring Program of the Port of San Diego, the conclusion was that there is zonal separation as regards the water temperature. In the northern part (off the Shelter Island – SI/1, number 1 in Figure 1a), the range is between 14°C and 19.5°C during the year and 17.5°C to 19.5°C during the summer. At the Laurel Street Anchorage (LSA/2, number 2 in Figure 1a), it reaches 21°C, with a range of 14°C to 21°C during the year but only 19°C to 21°C during the summer. Further south at the Bay Bridge Anchorage (BBA/3, number 3 in Figure 1a) the range is from 15°C to 22°C and again in the summer is from 20°C to 22°C. At the Sweet Water Channel (SWC/4, number 4 in Figure 1a) the range is from 14°C to 25°C with 22°C to 25°C in the summer. In Chula Vista Marina (CVM/5, number 5 in Figure 1a), it reaches a maximum of 26°C and a minimum of 23°C in the summer. As expected, the north part of the bay is colder than the south and in the summer the water is much

warmer than in the winter. The salinity varies from 32.5 to 37.5 ppt and the average is 35 ppt. The zonal separation is similar to the temperature. In LSA and SI, the range is from 33 to 35.5 ppt. In BBA, it reaches 36 ppt. In SWC, the range is from 32 to 37 ppt. In CVM, it is from 34 to 37.5 ppt. Again, detailed analysis shows that in the summer, salinity increases with an average of 1 ppt because of the zero precipitation. Therefore, 36 ppt is used as the standard salinity during the summertime.

6.2.4. Atmospheric Forcing

The winds have a very small effect on the currents because of their intensity and the geography of the Bay. Both mean westerly winds in the afternoon and mean easterly winds in the morning and evening are less than 5 m/s. According to NOAA's weather description, there are practically no storms for San Diego during June, July and August. Wind forcing is always less significant than tidal forcing. The shallow waters make instrument deployment problematic. With small currents, the angular momentum of the instruments induces direction errors. Hence, the model is more difficult to validate in these areas. Annual precipitation is about 0.26 m (Woodward and Clyde, 1996) and occurs mostly in winter. Therefore, in terms of estuarine classification, San Diego Bay is generally positive, i.e., drainage inflow exceeds evaporation (Pritchard, 1952). However, during the summer, the precipitation is usually zero. The evaporation rate, about 0.16 m, exceeds precipitation (Peeling, 1975) and a "reversed estuary" phenomenon is observed (Defant, 1961). In general, the low inflow of fresh water provokes very small buoyancy forcing; hence the density-driven circulation is driven by seasonal heating and evaporation. Note that for precipitation, in June, the rainfall is negligible averaging only 0.17 cm, in July 0.5 cm and in August 0.25 cm. Therefore, small surface water mass flux (mostly in winter) and wind forcing for the San Diego Bay are ignored. This study area is a small basin with circulation driven by tidal flow (Fagherazzi et al., 2003).

6.2.5. Water Quality Monitoring

In 1960, an earthquake with a Richter scale of 9 in Chile caused the biggest sudden rise in sea level ever recorded in the San Diego area of 1.07 m at the Scripps pier. There is a natural protection due to the 160 km wide continental shelf of San Diego. There is a fault off San Diego Bay, but it is inactive. These are the reasons why from the 15 locally generated tsunamis in California since 1812, only two have occurred in Southern California, and only one in San Diego, dating back to 1862.

Several mineral resource extraction activities are now occurring or have occurred in the recent past in San Diego Bay. Among them, the most important are the production of sodium chloride (salt), bromine and other chemicals from sea water, magnesium, magnesium compounds and brine. There is widespread toxicity in San Diego Bay sediments attributable to copper, zinc, mercury, polycyclic aromatic hydrocarbons, polychlorinated biphenyls (PCBs) and chlordane. No single chemical or chemical group has a dominant role in contributing to the identified toxicity. Contributions of trace metals from vessel activities have long been suspected as a potentially large source to San Diego Bay. Actually, Shelter Island Yacht Basin, a semi-enclosed boat harbor, has been added to the State's list of impaired water bodies (the 303d list). These contributions arise from specially formulated paints, impregnated with biocides, and applied to boat hulls to retard the growth of fouling organisms such as barnacles.

6.3. HYDRODYNAMIC MODEL

6.3.1. Model Description

The numerical hydrodynamic model implemented for San Diego Bay is a depth-averaged, boundary fitted tidal and residual circulation model known as WQMAP (Muin and Spaulding, 1996; 1997) developed at the Applied Science Associates Inc.. The numerical techniques incorporated in the model are well documented, thus only a summary of the model characteristics is presented. WQMAP is an integrated hydrodynamic and water quality modeling system designed for use within coastal and fresh water environments. This commercial off-the-shelf program was developed by Applied Science Associates, Inc. out of Narragansett, Rhode Island. WQMAP consists of three basic components: a boundary-fitted coordinate grid creation module, a three-dimensional hydrodynamics model, and a water quality or pollutant transport model. These models are executed on a boundary fitted grid system. They can also be operated on any orthogonal curvilinear grid or a rectangular grid, which are special cases of the boundary fitted grid. The model is configured to run in a vertically averaged (barotropic) mode or as a fully three-dimensional (baroclinic) mode. Several assumptions are made in the model formulation, including the hydrostatic (shallow water) approximation, the Boussinesq approximation, and incompressibility. In this study, the 2D version is used.

Most striking feature of WQMAP is its hybrid orthogonal curvilinear-terrain following coordinate system. Let (φ, λ, z) be the latitude, longitude, and height, and (ξ, η, σ) be a hybrid coordinate system with a generalized orthogonal curvilinear coordinate system (ξ, η) in the horizontal and terrain-following σ-coordinate in the vertical. The metric coefficients connecting (ϕ, λ) to (ξ, η) are defined by

$$g_{11} = (\frac{\partial \lambda}{\partial \xi})^2 \cos^2 \phi + (\frac{\partial \varphi}{\partial \xi})^2, \tag{1}$$

$$g_{22} = (\frac{\partial \lambda}{\partial \eta})^2 \cos^2 + (\frac{\partial \varphi}{\partial \eta})^2. \tag{2}$$

The coefficient g_{11} is the metric tensor in ξ-direction and the coefficient g_{22} metric tensor in η-direction. These tensors permit the model to transform the user defined boundary fitted grid to a numerical grid employed for spatial discretization utilized in an Arakawa *C* Grid.

Let (ζ, *H*) be the surface elevation and bathymetry. $D = H + \zeta$, is the total water depth. The σ- and z-coordinates are connected by

$$\sigma = \frac{z + H}{\zeta + H}, \tag{3}$$

which makes $\sigma = 1$ for the ocean surface and $\sigma = 0$ for the ocean bottom.

The 2D WQMAP represents a depth-averaged shallow-water system (similar to Wang et al., 1998). Let (U, V) be the vertically averaged velocity components in (ξ, η) directions. The momentum equations for (U, V) are given by

$$\frac{\partial UD}{\partial t} + \frac{1}{\sqrt{g_{11}g_{22}}}\left[\frac{\partial\left(U^2 D\sqrt{g_{22}}\right)}{\partial\xi} + \frac{\partial\left(UVD\sqrt{g_{11}}\right)}{\partial\eta} + UVD\frac{\partial\left(\sqrt{g_{11}}\right)}{\partial\eta} - V^2\frac{\partial\left(\sqrt{g_{22}}\right)}{\partial\xi}\right] - fDV$$
$$= -\frac{gD}{R\sqrt{g_{11}}}\left[\frac{\partial\zeta}{\partial\xi} + \frac{D}{\rho_0}\int_{-1}^{0}\int_{\sigma}^{0}\left(\frac{\partial\rho}{\partial\xi} - \frac{\sigma}{D}\frac{\partial D}{\partial\xi}\frac{\partial\rho}{\partial\sigma}\right)d\sigma\right] + \frac{1}{\rho_0}\left(\tau_\xi^w - \tau_\xi^b\right) + A_h D\nabla^2 U, \tag{4}$$

$$\frac{\partial VD}{\partial t} + \frac{1}{\sqrt{g_{11}g_{22}}}\left[\frac{\partial\left(UVD\sqrt{g_{22}}\right)}{\partial\xi} + \frac{\partial\left(V^2 D\sqrt{g_{11}}\right)}{\partial\eta} + UVD\frac{\partial\left(\sqrt{g_{22}}\right)}{\partial\xi} - U^2\frac{\partial\left(\sqrt{g_{11}}\right)}{\partial\eta}\right] + fDV$$
$$= -\frac{gD}{R\sqrt{g_{22}}}\left[\frac{\partial\zeta}{\partial\eta} + \frac{D}{\rho_0}\int_{-1}^{0}\int_{\sigma}^{0}\left(\frac{\partial\rho}{\partial\eta} - \frac{\sigma}{D}\frac{\partial D}{\partial\eta}\frac{\partial\rho}{\partial\sigma}\right)d\sigma\right] + \frac{1}{\rho_0}\left(\tau_\eta^w - \tau_\eta^b\right) + A_h D\nabla^2 V. \tag{5}$$

The continuity equation is represented by

$$R\sqrt{g_{11}g_{22}}\frac{\partial\zeta}{\partial t} + \frac{\partial\left(UD\sqrt{g_{22}}\right)}{\partial\xi} + \frac{\partial\left(VD\sqrt{g_{11}}\right)}{\partial\eta} = 0. \tag{6}$$

Here, R is the earth radius; ρ_0(= 1025 kg m^{-3}) is the characteristic density for the seawater; f is the Coriolis parameter; g is the acceleration due to gravity; A_h is the horizontal eddy viscosity; (τ_ξ^w, τ_η^w) are the wind stress; and (τ_ξ^b, τ_η^b) are the bottom stress. As with any depth-averaged model, it is implicitly assumed that velocity and density are nearly constant over the water column. However, horizontal density gradients are treated explicitly in the momentum equations. As we mentioned in Section 2 that the freshwater flow and surface winds in the bay are low. The currents in San Diego Bay are predominately produced by tides. Thus, the horizontal density gradient can be neglected in short-term prediction. A similar model popularly used in the coastal oceanographic community is the Princeton Ocean Model (POM). Chu et al. (2001, 2005) show the capability of POM for littoral prediction.

6.3.2. Model Implementation

WQMAP for San Diego Bay covers an area of 43 km^2. Different from Wang et al. (1998), the model domain is only The computational mesh has 150×200 (30,000) grid nodes with an average horizontal resolution of 40 m. Model bathymetry is determined from depth sounding data provided by NOAA and supplemented by data from published navigation charts. Recently Navy conducted bathymetry surveys show that the water depths in regions near the bay entrance are significantly deeper than the water depths shown on the NOAA navigation chart (Wang et al., 1998). The most up-to-date bathymetry data are used in the model.

Water surface elevation and velocity are set to zero, and temperature and salinity are assigned as the characteristic values for San Diego Bay (16^{o}C, 34 ppt) at all grid points. The model is allowed to "spin up" from quiescent initial condition for one day before any model results are used for analysis. A six-minute time step is chosen for time step. At this time step the CFL condition is satisfied. Besides, the model parameters are given as follows: the wind drag coefficient (0.0014), the bottom drag coefficient (0.003), the vertical viscosity (0.005 m^2s^{-1}), the vertical diffusivity (0.001 m^2s^{-1}), and the horizontal diffusivity (1.0 m^2s^{-1}).

6.3.3. Tidal Forcing

Temporally varying sea surface elevation (or tidal harmonic constituents) along the open boundary (entrance of San Diego Bay) is taken as the model forcing function. Such data are available at the NOAA Center for Operational Oceanographic Products and Services website. In order to verify the model performance using the ADCP data shown in Figure 3, the elevation data with six-minute interval are archived from time 0000 on 22 June 1993 to 2354 on 27 August 1993 for San Diego Bay entrance, in accordance with NOAA San Diego Station number 9410170, located at (32^{o}42'48"N, 117^{o}10'24"W).

6.3.4. Model Verification

Statistical analysis shows that a good correlation exists between most of the compared signals in both phase and amplitude (correlation coefficient above 90% in all cases). For nb1, the u speed between the data and the model has a correlation coefficient of 91.87% and can be verified. The observational u-velocity ranges between -51.8 and 44.5 cm/s and the modeled u-velocity changes between -46.9 and 40.8 cm/s (Figure 4). The difference between the observational and modeled mean u-velocity is 0.49 cm/s. Furthermore, the root mean square error (between model and observation) is 9.02 cm/s. For nb1, the v speed between the data and the model has a correlation coefficient of 91.66% and can be verified optically. The observational v-velocity ranges between -31.6 and 29.6 cm/s and the modeled v-velocity changes between -37.0 and 32.0 cm/s. The difference between the observational and modeled mean v-velocity is -0.65 cm/s. The root mean square error of v-velocity is 6.83 cm/s.

For nb2, the u speed between data and model has a correlation coefficient of 92.60% and can be verified optically. The observational u-velocity ranges between -42.8 and 32.8 cm/s and the modeled u-velocity changes between -40.2 and 34.3 cm/s. The difference between the observational and modeled mean u-velocity is 1.0862 cm/s. Furthermore, the root mean square error (between model and observation) is 6.7356 cm/s. For nb1, the v speed between the data and the model has a correlation coefficient of 92.60 % and can be verified optically. The observational v-velocity ranges between -34 and 42.7 cm/s and the modeled v-velocity changes between -20.4 and 23.5 cm/s. The difference between the observational and modeled mean v-velocity is -1.2971. The root mean square error of v-velocity is 8.5035.

Comparison of the current speed between observation and the model is acceptable. As regards the point south of Coronado Island (bb), when filtering the data to keep only the part that results from the tidal influence, an improved correlation between the model and observation occur. Again, a band-pass butterworth filter is first applied to filter out all

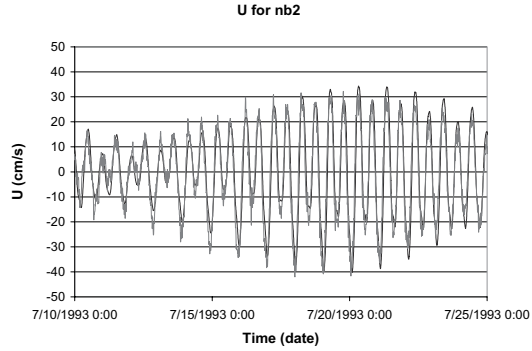

(a)

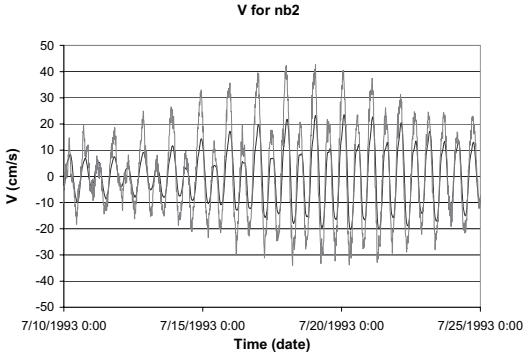

(b)

Fig. 4. Model (solid curve) and (ADCP) data (dashed curve) comparison for station-nb1: (a) u-component, and (b) v-component.

frequencies either smaller than 0.5 cycles per day or greater than 2.5 cycles per day. The correlation coefficient is 85.09% for u-velocity and 78.49% for v-velocity. Optically, the amplitude difference between the model and observation improves as well. Thus, it is possible to conclude that by filtering the results of the non-tidal influence, a 2-D model can be used in the entrance of San Diego Bay with relatively better results. The middle and upper levels contribute much more to the vertical average u component of bb than the lower (to bottom) depths and indicate its behavior much better. Actually the correlation coefficient of the average u component and the surface u is 91.63% and between the average u component and the middle depth u is even higher (92.14%). Moreover, the middle depth represents the u component better since it has also a smaller, relative mean error (RME), root mean square error (RMSE), and the error coefficient of variation (ecv),

$$\mathrm{RME} = \frac{\sum_{i=1}^{n}(X_i^{\mathrm{mod}} - X_i^{obs})^2}{\sum_{i=1}^{n}\left|X_i^{\mathrm{mod}}\right|^2},\ \mathrm{RMSE} = \sqrt{\frac{1}{n}\sum_{i=1}^{n}(X_i^{\mathrm{mod}} - X_i^{obs})^2}\quad ECV = \frac{RMSE}{\sqrt{\frac{1}{n}\sum_{i}\left|X_i^{\mathrm{mod}}\right|^2}}, \tag{7}$$

where $\left(X_i^{mod}, X_i^{obs}\right)$ are the modeled and observational data.

The bottom u component and the average u have a correlation coefficient of only 62.22%. For the v component, the correlation between the average and the v component in all depths is high: For bottom, the correlation coefficient is 96.24%, for surface 99.26%, and again for middle depth, it is the best with a coefficient of 99.43% and better rme, rmse and ecv than the other cases. In order to evaluate the model further, the water elevation in position nb2 is calculated and despite the fact that exact verified data is not available, an attempt will be made to compare it in two different ways. First, Table 2 describes all results after harmonic decomposition.

Table 2. Harmonic decomposition of the modeled results.

TIDE	FREQ	AMPL	AMP.ERR	PHASE	PH ERR	SNR
MSF	0.0028219	0.0061	0.014	266.81	160.24	0.2
*2Q1	0.0357064	0.0067	0.003	337.90	21.94	6.8
*Q1	0.0372185	0.0364	0.002	76.81	4.66	2.4e+002
*O1	0.0387307	0.1952	0.003	125.14	0.86	5e+003
*NO1	0.0402686	0.0096	0.003	19.17	16.04	13
*K1	0.0417807	0.3773	0.002	60.54	0.44	2.5e+004
J1	0.0432929	0.0026	0.002	97.99	69.16	1.2
*OO1	0.0448308	0.0157	0.002	129.23	9.23	40
*UPS1	0.0463430	0.0047	0.003	289.53	32.85	2.7
*N2	0.0789992	0.1226	0.014	203.96	7.74	75
*M2	0.0805114	0.5804	0.015	270.27	1.36	1.6e+003
*S2	0.0833333	0.2144	0.013	267.04	3.93	2.6e+002
ETA2	0.0850736	0.0077	0.011	7.45	98.73	0.48
*MO3	0.1192421	0.0042	0.001	258.54	22.76	8.5
*M3	0.1207671	0.0021	0.001	172.85	40.42	2.4
*MK3	0.1222921	0.0085	0.001	219.46	10.21	33
*SK3	0.1251141	0.0026	0.001	208.56	32.29	3.7
*MN4	0.1595106	0.0039	0.002	15.82	21.09	6.1
*M4	0.1610228	0.0107	0.001	75.84	8.11	71
*MS4	0.1638447	0.0074	0.002	71.22	11.13	23
S4	0.1666667	0.0014	0.001	66.29	51.91	1.2
*2MK5	0.2028035	0.0037	0.001	185.30	24.66	6.6
2SK5	0.2084474	0.0003	0.001	258.37	225.54	0.057
2MN6	0.2400221	0.0029	0.002	355.66	52.92	1.5
*M6	0.2415342	0.0059	0.002	52.23	22.32	6.5
*2MS6	0.2443561	0.0080	0.003	72.33	18.29	10
2SM6	0.2471781	0.0019	0.002	83.37	75.50	0.65
*3MK7	0.2833149	0.0042	0.002	108.25	31.28	3.4
*M8	0.3220456	0.0007	0.000	295.35	30.49	3.3

To compare the model results with a previous study (Wang et al., 1998), the four main tidal constituents (K1, O1, S2, M2) at downtown (further north and deeper than the nb2 position) are used. Amplitude difference (model minus observation) is 3.83 cm for M_2 (but only 1.08 cm, if compared to that of south San Diego), 3.73 cm for K_1, -2.19 cm for O_1, and 1.1 cm for S_2. Phase difference is 1.71° for M_2, 25.94° for K_1, 45.33° for O_1, and 5.41° for

S_2. Differences in bathymetry and analysis can justify such small discrepancies, especially since there is no certainty about the position for which the data was collected.

The best choice for a valid comparison is to compare the model results at nb2 with the NOAA San Diego station at the pier. The data is gathered too close to land, and therefore, cannot be exactly compared. However, it can be compared with a point very near the actual San Diego Station position. Amplitude difference (model minus observation) is 2.51 cm for M_2, 0.94 cm for K_1, 0.84 cm for O_1, and 0.71 cm for S_2. Phase difference is 0.75^o for M_2, 26.08^o for K_1, 29.58^o for O_1, and 48.96^o for S_2. Again, it can be stated that differences in bathymetry and analysis can justify such small discrepancies, especially since there is no precision about the position for which the data was compared. The results from this more accurate comparison are even better than the previous one.

Overall, the model results are reasonably good, especially taking into account that the comparison between data and model is not at exactly the same position and the proximity of the ADCPs to the shore. If finer grid and more accurate bathymetry are used, the model results may be further improved.

6.4. CHEMICAL SPILL MODEL

6.4.1. Model Description

A chemical spill model, called CHEMMAP and developed at developed at the Applied Science Associates Inc., is used to predict the trajectory and fate of floating, sinking, evaporating, soluble and insoluble chemicals and product mixtures. It estimates the distribution of chemical elements (as mass and concentrations) on the surface, in the water column and in the sediments. The model is 3D, separately tracking surface slicks, entrained droplets or particles of pure chemical, chemical adsorbed to suspended particulates, and dissolved chemical (McCay and Isaji, 2002). The CHEMMAP model is used to predict the propagation of chemicals.

CHEMMAP can be either run as a certain scenario with tidal and wind forcing or in stochastic mode to estimate the probable distribution and concentrations resulting from hypothetical spills. In this study, CHEMMAP was used to predict the chemical spill in San Diego Bay. Therefore, the physical characteristics (such as velocity, temperature, salinity) of this tidally dominated bay are simulated using WQMAP. It incorporates a number of model components including simulation of the initial release for surface and subsurface spills, slick spreading, transport of floating, dissolved and particulate materials, evaporation and volatilization, dissolution and adsorption, sedimentation and degradation. It uses physical and chemical properties such as density, viscosity, vapor pressure, surface tension, water solubility, environmental degradation rates, and adsorbed/dissolved partitioning coefficients. The Stoke's Law is used to calculate vertical velocities. Furthermore, its approach towards propagation is Langrangian. The outputs of the model include the trajectories, and concentrations. More specifically, it is possible to see the swept area by a floating chemical, as well as the total, absorbed, dissolved and particulate concentration in both the water column and the sediments. The most important is that it is then possible to determine the range of distances and directions of the contamination caused from the spill at a particular location.

6.4.2. Model Initialization

The model is initialized for the spilled mass at the location and depth of the release. The state and solubility are the primary determining factors for the initialization algorithm. If the chemical is highly soluble in water and is either a pure chemical (e.g., the benzene scenario) or dissolved in water (e.g., the methanol scenario), the chemical mass is initialized in the water column in the dissolved state and in a user-defined initial volume. For insoluble or semi-soluble gases released underwater (e.g., the naphthalene gas scenario), the spilled mass is initialized in the water column at the release depth in a user-defined plume volume, as bubbles. The median particle size is characterized by a user-defined diameter (McCay and Isaji, 2002).

For the state where the chemical of interest is both adsorbed to particles and dissolved in the water phase of the bulk liquid (e.g. our ammonia liquefied gas scenario), dissolved mass is also initialized in the initial plume volume. The mass of chemical spilled is corrected from the bulk spill volume using the appropriate density and concentration data from the database (McCay and Isaji, 2002).

Chemical mass is transported in three-dimensional space and time, by surface wind drift, other currents, and vertical movement in accordance with buoyancy and dispersion. The model simulates adsorption onto suspended sediment, resulting in sedimentation of material. Stoke's Law is used to compute the vertical velocity of pure chemical particles or suspended sediment with adsorbed chemical. If rise or settling velocity overcomes turbulent mixing, the particles are assumed to float or settle to the bottom. Settled particles may later re-suspend (assumed to occur above 20 cm/s current speed). Wind-driven current (drift) in the surface water layer (down to 5m) is calculated within the fates model, based on hourly wind speed and direction data. Surface wind drift of oil has been observed in the field to be 1-6% of wind speed in the direction of 0-30 degrees to the right (in the northern hemisphere) of the down-wind direction (Youssef and Spaulding, 1993). The user may also specify the wind drift speed and angle (McCay and Isaji, 2002).

CHEMMAP simulates degradation, volatilization, evaporation, dissolution, entrainment and spreading. More specifically, spreading is simulated using the Fay algorithm (Fay, 1971). Entrainment is modeled as for oil (Delvigne and Sweeney, 1988). Surface floating chemicals interaction with shorelines is simulated based on the algorithms developed for oil spills (French et al., 1999). The dissolution rate of pure chemicals is a function of solubility using a first order constant rate equation. The dissolved chemical in the water column is assumed to adsorb to particulate matter in accordance with the equilibrium partitioning theory (DiToro et al., 1991). Evaporation is modeled following the theory that the rate of mass flux to the atmosphere increases with vapor pressure, temperature, wind speed and surface area (Mackay and Matsugu, 1973). Volatilization from the water column is calculated from the chemical's vapor pressure and solubility (Lyman et al., 1982). Degradation is estimated assuming a constant rate of "decay" specific to the environment where the mass exists (i.e., atmosphere, water column or sediment).

The spilled chemical is modeled using the Lagrangian approach. At each time step, phase transfer rates (evaporation, dissolution, volatilization, and entrainment) are calculated and a proportionate percentage of the spillets are transferred to the new phase (McCay and Isaji, 2002).

6.5. CHEMICAL POLLUTANTS

The choice of the chemicals used in this study is based on chemical/physical properties and toxicity data and are contained in a database compiled from published literature sources, mainly French et al. (1996) and Mackay et al. (1992a, b, c, d). Since several properties vary with temperature, the chemical data are for an initial temperature of 25^{o}C. The model corrects these parameters to the ambient temperature for the spill incident. The algorithms for changing viscosity and vapor pressure to ambient temperature are taken from French et al. (1996), who developed regression using the data in Gambill (1959). For pure chemical processes, the increase per 10^{o}C is assumed to be a factor of 2. For biological processes (e.g., degradation rates), the increase in rate per increase of 10^{o}C is assumed to be a factor of 3 (McCay and Isaji, 2002). Table 3 shows the comparison of the chemicals selected for this study.

Table 3. Comparison of chemicals used in the chemical spill scenarios.

	Methanol	Benzene	Ammonia	Chlorobenzene	TCE	Naphthalene (gas)
Floatation	Floater	Floater	Floater	Sinker	Sinker	Sinker/ Air dispersed
Solubility	High	High	High	Normal	High	Semi
Volatility	High	High	High	Semi	Semi	None
Absorption	Dissolves	Moderate	Slight	Moderate	Moderate	Moderate
Flammability	High	High		High		High
Water/Air rapid interaction	No	No		No		No

6.5.1. Floating Chemicals

Methanol (CH3OH) is a colorless fairly volatile liquid, belonging to the aliphatic alcohols chemical type. It is originally distilled from wood, but currently, it is synthetically produced from carbon oxides and hydrogen. It has a faintly sweet pungent odor like that of ethyl alcohol. It has a flash point 12.222^{o}C and its density is 791 kg/m^{3} (at 25^{o}C). Its vapors are slightly heavier than air and may travel some distance to a source of ignition and flash back. Any accumulation of vapors in confined spaces, such as buildings or sewers, may explode if ignited, so it is very dangerous. It is used to make chemicals, to remove water from automotive and aviation fuels, as a solvent for paints and plastics, as an alternative motor fuel and as an ingredient in a wide variety of products, so it is not easy control. Actually, the most recent inventory is estimated to be 1,125 metric tons in the U.S. alone.

Methanol reacts violently with acetyl bromide. Mixtures with concentrated sulfuric acid and concentrated hydrogen peroxide can cause explosions. It reacts with hypochlorous acid either in water solution or mixed water/carbon tetrachloride solution to give methyl

hypochlorite, which decomposes in the cold and may explode on exposure to sunlight or heat. It gives the same product with chlorine and can react explosively with isocyanates under basic conditions. The presence of an inert solvent mitigates this reaction. A violent exothermic reaction occurred between methyl alcohol and bromine in a mixing cylinder. A flask of anhydrous lead perchlorate dissolved in methanol exploded when it was disturbed.

Hence, methanol is high flammable, is a floater, is highly volatile, is highly soluble and remains dissolved. Furthermore, is a toxic element, and therefore, very dangerous. Its immediately dangerous to life or health indicator (IDLH) is very high (6,000 ppm), its short term exposure limit (STEL) is 250 ppm and its odor threshold is 4.2 ppm. Its degradation rate is 0.097835 (%/day) in air and sediments and 0.3024 (%/day) in water.

Even though it is not "acutely" toxic, inhalation can cause cough, dizziness, headache, nausea, weakness and visual disturbance. Ingestion can be even worse causing abdominal pain, convulsions, shortness of breath, unconsciousness and vomiting. However, what is more important is its ecotoxicity. For certain fish (such as red drums), shrimps, mussels and snails, it can be lethal. Benzene (C6H6) is the second chemical to be used. It is also toxic, causing the same symptoms as methanol, and can be fatal to many species in the eco system including all the aforementioned ones as well as oysters, clams, trout, salmon, catfish and goldfish. As regards its toxicity, benzene is a confirmed carcinogen, develops and reproduces toxins, and therefore, is extremely dangerous. The water maximum contaminant level is 0.000005 kg/m^3. Its immediately dangerous to life or health indicator (IDLH) is not as high as methanol (500 ppm), its short term exposure limit (STEL) is 2.5 ppm and its odor threshold is 34 ppm for detection and 97 ppm for recognition. Its degradation rate is 0.97835 (%/day) in air, 0.097835 (%/day) in water and 0.0097835 (%/day) in sediments.

For chemical characteristics, benzene is high flammable, floater, highly volatile, highly soluble, and moderately absorbable to particles. It is a clear colorless liquid with a petroleum-like odor. It is less dense than water (0.877 g/cm^3) and slightly soluble in water. Its vapors are heavier than air. Benzene reacts vigorously with alkyl chloride or other alkyl halides even at -70^{o}C in the presence of ethyl aluminum dichloride or ethyl aluminum sesquichloride and explosions have been reported. It ignites in contact with powdered chromic anhydride. It is incompatible with oxidizing agents such as nitric acid. Mixtures with bromine trifluoride, bromine pentafluoride, iodine pentafluoride, iodine heptafluoride and other interhalogens can ignite upon heating.

The ammonia (NH3) liquefied gas is clear and colorless and has a strong odor. It is shipped as a liquid under its own vapor pressure. Its density in the liquid form is 12.8825 kg/m^3. Contact with the unconfined liquid can cause frostbite. Gas generally regarded as nonflammable but does burn within certain vapor concentration limits and with strong ignition. Fire hazard increases in the presence of oil or other combustible materials. Although gas is lighter than air, vapors from a leak initially hug the ground. Prolonged exposure of containers to fire or heat may cause violent rupturing and rocketing. Long-term inhalation of low concentrations of the vapors or short-term inhalation of high concentrations has adverse health effects. It is used as a fertilizer and refrigerant, and in the manufacture of other chemicals

Ammonia is a floater, highly volatile, highly soluble and slightly absorbable to particles, and reacts exothermically with all acids. Violent reactions are possible. It also readily combines with silver oxide or mercury to form compounds that explode on contact with halogens. When in contact with chlorates, it forms explosive ammonium. As for toxicity, its immediately dangerous to life or health indicator (IDLH) is relatively small (300 ppm), its short term exposure limit (STEL) is 35 ppm and its odor threshold is 0.019

ppm. Its degradation rate is 0.1586 in both air and water. Contact with ammonia could cause skin and eye burns and inhalation some burning sensation, cough, shortness of breath and sore throat. For the ecosystem, its slight toxicity can be lethal to shrimp, prawns, salmon, trout and catfish.

6.5.2. Sinking Chemicals

Chlorobenzene (C6H5Cl) is a sinking chemical. It is a colorless to clear, yellowish liquid with a sweet almond-like odor. It is insoluble in water and a little denser than water (1,107 kg/m^3). Its vapors are heavier than air. It is used to make pesticides, dyes, and other chemicals Chlorobenzene undergoes a sometimes explosive reaction with powdered sodium or phosphorus trichloride and sodium. It may react violently with dimethyl sulfoxide. It reacts vigorously with oxidizing agents. It attacks some forms of plastic, rubber and coatings and it forms a shock sensitive solvated salt with silver perchlorate. Chlorobenzene is, therefore, a sinker, semi-volatile, soluble, highly flammable and moderately absorbable to particles. For toxicity, its immediately dangerous to life or health indicator (IDLH) is quite big (1,000 ppm), and its odor threshold is 1.3 ppm. Its degradation rate is 0.09784 (%/day) in Air, 0.0097835 (%/day) in Water and 0.00098 (%/day) in Sediments. Inhalation of chlorobenzene can cause drowsiness, headache, nausea and unconsciousness. Ingestion causes abdominal pain. As regards eco-toxicity, it can be lethal to prawns, trout and goldfish.

Another sinker is trichloroethylene (C2HCl3). It is a toxic sinker with similar results as chlorobenzene when in contact with humans. Furthermore, it is a proven carcinogen. It is a clear colorless volatile liquid having a chloroform-like odor. It is denser than water, slightly soluble in water and is non-combustible. It is used as a solvent, fumigant, in the manufacture of other chemicals, and for many other uses. It has been determined experimentally that mixtures of finely divided barium metal and a number of halogenated hydrocarbons possess an explosive capability. Specifically, impact sensitivity tests have shown that granular barium in contact with monofluorotrichloromethane, trichlorotrifluoroethane, carbon tetrachloride, trichloroethylene, or tetrachloroethylene can detonate. It has been determined experimentally that a mixture of beryllium powder with carbon tetrachloride or with trichloroethylene will flash or spark on heavy impact. A mixture of powdered magnesium with trichloroethylene or with carbon tetrachloride will also flash or spark under heavy impact. Thus, trichloroethylene is a sinker, semi-volatile, highly soluble and moderately absorbable to particles. As regards toxicity, its immediately dangerous to life or health indicator (IDLH) is the same as chlorobenzene (1,000 ppm), its short term exposure limit (STEL) is 100 ppm and its odor threshold is 82 ppm. Its degradation rate is 0.09784 (%/day) in air, 0.03024 (%/day) in water and 0.003024 (%/day) in sediments. Its dangers for the eco-system include death to toads, trout and flagfish.

6.5.3. Gaseous Chemicals

Naphthalene (C10H8) is a gas chemical. It is a dark liquid mixture, with much different qualities than all the previous chemicals. It is insoluble in water and denser than water. A part disperses in the atmosphere and another sinks in water. Contact with naphthalene may cause irritation to skin, eyes, and mucous membranes. It can cause confusion, headache, sweating, nausea, vomiting and jaundice when inhaled. It is toxic by ingestion and can cause abdominal pain, convulsions, diarrhea, dizziness and unconsciousness. Its toxicity is

moderate and immediately dangerous to life or health indicator (IDLH) is 250 ppm, its short term exposure limit (STEL) is 15 ppm and its odor threshold is 0.038 ppm. It is a known carcinogen, and therefore, dangerous to humans. A mixture containing naphthalene may react vigorously with strong oxidizing agents. It can also react exothermically with bases and with diazo compounds. Naphthalene reacts violently with chromic anhydride. Hence, naphthalene disperses in the atmosphere (but can be also a sinker), is not volatile, is semi-to non-soluble, moderately absorbable to particles, is highly flammable and does not react rapidly with either water or air. Its degradation rate is 0.97835 (%/day) in air, 0.09784 (%/day) in water and 0.00302 (%/day) in sediments. Its dangers for the eco-system include the death of toads, crabs, shrimp, cod, salmon, trout and oysters, being one of the most dangerous enemies of natural underwater life.

6.6. CHEMICAL SPILL PATTERNS

The coupled WQMAP-CHEMMAP is used to investigate the chemical spill patterns for floating, sinking, gaseous chemicals. Since the WQMAP is integrated for the period from 0000 on 22 June 1993 to 2354 on 27 August 1993 for San Diego Bay, the following scenarios were suggested: A small boat drops one barrel of chemical (methanol, …) in less than 12 minutes on midnight July 4, 1993 (Independence Day) at (1) northern San Diego Bay (32^{o}43'N, 117^{o}13.05' W) (Point 2 in Figure 1a) , and (2) southern San Diego Bay (32^{o}39'N, 117^{o}07.92' W) (Point 4 in Figure 1a). The release depth is 1 m and the initial plum thickness is 0.5 m. Two distinct spill patterns are found for all the chemicals. Here, spill of methanol is presented for illustration.

6.6.1. Pollutants Released at North San Diego Bay

The chemical spill pattern is described as follows. In 3 hours, the methanol is in San Diego port (Figure 5a) and in 10 hours it is spread all over the North San Diego Bay. However, the south part of the Bay is contaminated much later. After two days, there are no pollutant particles south of 32^{o}40'N (Figure 5b). After 3 days the northern part is heavily impacted but after 9 days, there are still no pollutant particles south of 32^{o}39'N. The methanol reaches the south end of the Bay only after 20 days (Figure 5c), but its concentration in the water column can be neglected. Figure 6 shows the swept area after 2 days and 32 days. In such a case, it can be concluded that there is plenty of time to take protective measures for the southern part of the Bay where the results of such an incident would be minimal.

Furthermore, after five entire days, one third of the methanol is still in the water column (Figure 7). Note that it takes almost 12 days for the concentration in the water column to reach 10% and 15 days for the decayed methanol to reach a level of 80%. Moreover, the end-state is the contamination not only of the San Diego Bay but also a considerable part of the sea outside the Bay. The scenario is repeated by increasing the amount of methanol, but nothing changes fundamentally. The mass balance curves and the area contaminated remain the same.

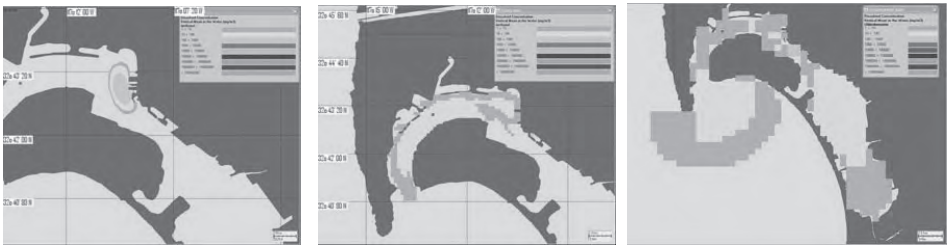

(a) (b) (c)

Fig. 5. Dissolved concentration in San Diego after (a) 3 hours, (b) 2 days, and (c) 20 days after methanol dropped in North San Diego Bay.

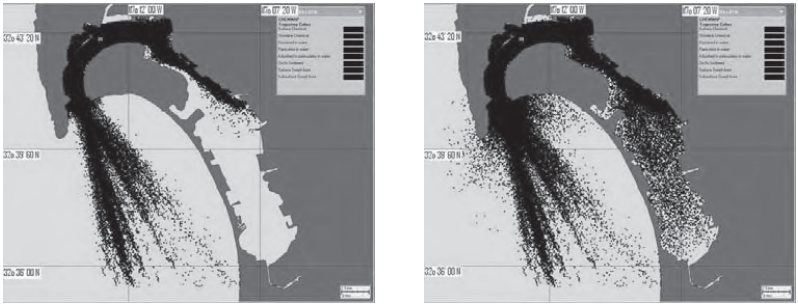

(a) (b)

Fig. 6. Swept area after (a) 2 days and (b) 32 days for methanol dropped in North San Diego Bay.

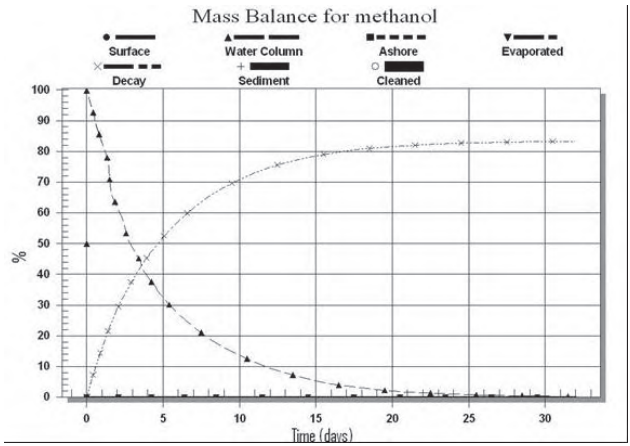

Fig. 7. Mass balance for methanol dropped in North San Diego Bay.

6.6.2. Pollutants Released at South San Diego Bay

The chemical spill pattern is described as follows. In 13 hours, the methanol reaches the central San Diego Bay (Figure 8). But, very few pollutants reach 32°41'N parallel. Figure 9 shows the swept area after 32 days. It is crucial for protective measures to highlight this fact because a chemical attack in the South San Diego Bay will have minimal effects, or at least much less considerable than an attack (or accident) in the north part of the bay. Figure 10 shows a similar but different result as regards the mass balance curves. Thus, the decayed methanol reaches 80% in only nine days, mainly due to the inert nature of methanol in combination to the shallow bathymetry of the southern part of the Bay. It is important to single out that in the first case (methanol spill over in the north), the dissolved concentration disappears after only 15 days, but in the second case (south), it needs 29 days. It is noted that the ecological catastrophe that can be caused with a relatively big amount of methanol spill over is very considerable, especially if the spill over is in the north. It can also be harmful to humans.

Fig. 8. Dissolved concentration in San Diego after 13 hours after methanol dropped in South San Diego Bay.

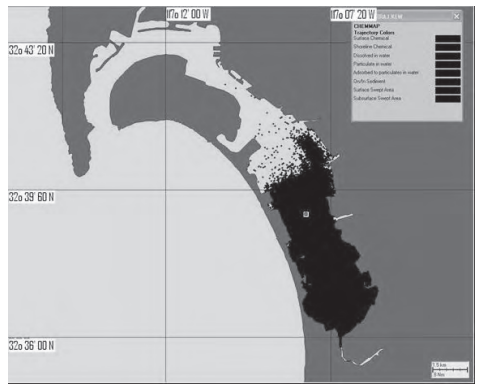

Fig. 9. Swept area after 32 days for methanol dropped in South San Diego Bay.

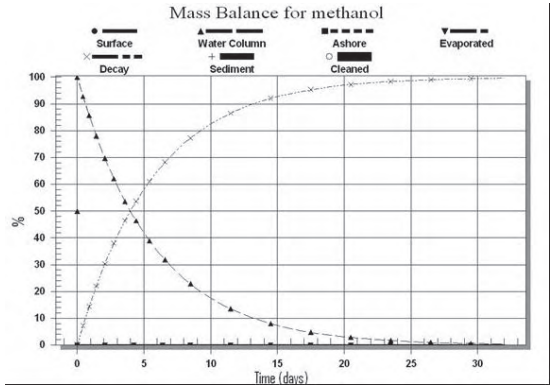

Fig. 10. Mass balance for methanol dropped in South San Diego Bay.

6.7. CONCLUSIONS

This study shows the vulnerability of a semi-enclosed tidal basin in a possible chemical attack or accident, with the aforementioned particular results for San Diego Bay. In order to summarize these results, it should be repeated that in a case of a chemical attack or accident, first the sensitive eco-system would be severely damaged, no matter the nature of the event and the location. If the chemical were a sinker, the results would be more catastrophic than if it were a floater. Since the water exchange with the Pacific Ocean occurs only through a narrow entrance, the water would be contaminated for long time.

Two regimes of the chemical dispersion were found in this thesis. The first was the case of an attack/accident in the North San Diego Bay. In that case the entire Bay would be contaminated. In 3 hours the chemical would reach San Diego port and city, in 12 hours the entire northern part of the Bay would be affected and in 2-5 days the south part of the bay would be contaminated as well. The rest of the Bay would be reached much later. The second regime was an attack/accident in the South San Diego Bay. In such case, the incident would have minimal effects on the city and the shores of Coronado Island (located in the north part of the bay) and none outside the Bay. On the other hand, when the spill occurs in the southern part of the Bay, a larger percentage of the chemical remains in the water column and for longer period of time, which makes it more "effective", which in a case of a chemical attack means lethal.

For the aforementioned reasons, the propagation model shows that the northern part of the Bay is more likely to be a target because it would affect the city, and it would reach, even slightly, the South San Diego Bay and would spread outside the Bay as well. In general, results concerning San Diego Bay can also be applied to studies in other semi-closed, barotropic, no-wind driven circulation basins.

As regards recommendations for future research, it should be mentioned that the use of more accurate bathymetry and of a finer grid would give better results in a similar case. Moreover, the use of more recent ADCP measurements, during a longer period of time would further improve the results and verify the overall conclusions. It would be helpful if the ADCPs used in the future were located in a bigger distance from the shore.

A more detailed comparison of 3D vs. 2D model is encouraged, as well as its application for drift and for instantaneous current prediction. Last but not least, as regards

chemical propagation, a classified research with data unavailable to foreigners about real chemical threats (e.g. anthrax) should be conducted.

ACKNOWLEDGMENTS

This work was funded by the Naval Oceanographic Office, the Office of Naval Research, and the Naval Postgraduate School.

REFERENCES

Chadwick, D. B., and Largier, J. L., 1999a. Tidal Exchange at the Bay-Ocean Boundary. Journal of Geophysical Research 104 (C12): 29,901-29,924.

Chadwick, D. B., and Largier, J. L., 1999b. The Influence of Tidal Range on the Exchange Between San Diego Bay and the Ocean. Journal of Geophysical Research 104 (C12): 29, 885-29, 899.

Cheng R. T., Casulli, V. T., and Gartner, J. W., 1983. Tidal, Residual, Inter-tidal Mudflat (TRIM) Model and its Applications to San Francisco Bay, California. Estuarine, Coastal and Shelf Science 36: 235-280.

Chu, P.C., Lu, S. H., and Chen, Y. C., 2001. Evaluation of the Princeton Ocean Model using the South China Sea Monsoon Experiment (SCSMEX) Data. Journal of Atmospheric and Oceanic Technology 18: 1521-1539.

Chu, P.C., C.-L. Fang,and C.S. Kim, 2005b. Japan/East Sea model predictability. Continental Shelf Research, 25, 2107-2121.

Defant, A, 1961. Physical Oceanography, New York, Pergamon Press.

Delvigne, G. A. L., and Sweeney, C. E., 1988. Natural Dispersion of Oil. Oil and Chemical Pollution 4: 281-310.

DiToro, D. M., Zarba, C. S., Hansen, D. J., Berry, W. J., Swartz, R. C., Cowan, C. E., Pavlou, S. P., Allen, H. E., Thomas, N. A., and Paquin, P. R., 1991. Annual Review: Technical Basis for Establishing Sediment Quality Criteria for Nonionic Organic Chemicals Using Equilibrium Partitioning. Environmental Toxicology and Chemistry 10: 1541-1583.

Fagherazzi Sergio, Patricia, L. Wiberg and Alan D. Howard, 2003. Tidal Flow in a Small Basin. Journal of Geophysical Research 108(C3): 16-1 to 16-10.

Fay, J. A., 1971. Physical Processes in the Spread of Oil on a Water Surface. Proceedings at Joint Conference and Control of Oil Spills, Washington, D.C., June 15-17, 1971.

Fischer H. B., List, E. J., Koh, R. C. Y., Imberger, J., and Brooks, N. H., 1979. Mixing in Inland and Coastal Waters. Academic Press, p. 483, San Diego.

French, D., Reed, M., Jayko, K., Feng, S., Rines, H., Pavignano, S., Isaji, T., Puckett, S., Keller, A., French III, F. W., Gifford, D., McCue, J., Brown, G., MacDonald, E., Quirk, J., Natzke, S., Bishop, R., Welsh, M., Phillips, M., and Ingram, B.S., 1996. The CERCLA Type A Natural Resource Damage Assessment Model for Coastal and Marine Environments (NRDAM/CME). Technical Documentation, Vol. I -VI, Final Report, submitted to the Office of Environmental Policy and Compliance, U.S. Dept. of the Interior, Washington, D.C., Contract No. 14-0001-91-C-11. April 1996.

French McCay, D. P., and Isaji, T., 2002. Evaluation of the Consequences of Chemical Spills Using Modeling: Chemicals Used in Deepwater Oil and Gas Operations. International Marine Environmental Seminar 2001, Journal of Marine Systems, Special Issue 2002.

Gambill, W. R., 1959. How to calculate liquid viscosity without experimental data. Chemical Engineering, p. 127.

Jackson J. A. and C. D. Winant, 1983. Effect of a Kelp Forrest on Coastal Currents. Continental Shelf Research 2(1): 75-80.

Lyman, C. J., Reehl, W. F., Rosenblatt, D. H., 1982. Handbook of Chemical Property Estimation Methods. McGraw-Hill Book Co., New York.

Mackay, D., and Matsugu, R. S., 1973. Evaporation Rates of Liquid Hydrocarbon Spills on Land and Water. The Canadian Journal of Chemical Engineering 51: 434-439.

Mackay, D., Shiu, W. Y., and Ma, K. C., 1992a. Monoaromatic Hydrocarbons, Chlorobenzenes, and PCBs. Illustrated Handbook of Physical-Chemical Properties and Environmental Fate for Organic Chemicals, Vol. I. Lewis Publishers, Chelsea, Michigan, 668p.

Mackay, D., Shiu, W. Y., and Ma, K. C., 1992b. Polynuclear Aromatic Hydrocarbons, Polychlorinated Dioxins, and Dibenzofurans. Illustrated Handbook of Physical-Chemical Properties and Environmental Fate for Organic Chemicals, Vol. II. Lewis Publishers, Chelsea, Michigan, 566p.

Mackay, D., Shiu, W. Y., and Ma, K. C., 1992c. Volatile Organic Chemicals. Illustrated Handbook of Physical-Chemical Properties and Environmental Fate for Organic Chemicals, Vol. III. Lewis Publishers, Chelsea, Michigan, 885p.

Mackay, D., Shiu, W. Y., and Ma, K. C., 1992d. Oxygen, Nitrogen, and Sulfur Containing Compounds. Illustrated Handbook of Physical-Chemical Properties and Environmental Fate for Organic Chemicals, Volume IV. Lewis Publishers, Chelsea, Michigan, 930p.

Madala, R. V., and Piaczek, S. A., 1977. A Semi-Implicit Numerical Model for Baroclinic Oceans. Journal of Computational Physics 23: 167-168.

Muin, M., and Spaulding, M. L., 1996. Two-Dimensional Boundary Fitted Circulation Model in Spherical Coordinates. Journal of Hydraulic Engineering 122 (9): 512-520.

Muin, M., and Spaulding, M. L., 1997. Three-Dimensional Boundary Fitted Circulation Model. Journal of Hydraulic Engineering 123 (1): 2-12.

Peeling, T. J., 1975. A Proximate Biological Survey of San Diego Bay, California. Naval Undersea RD Center, San Diego, California, Technical Report No. TP389.

Pritchard, D. W., 1952. Estuarine Hydrography. Advances in Geophysics, Academic Press, pp. 342-280.

Spaulding, M.L., Mendelsohn, D.L., and Swanson, J.C., 1999. WQMAP: An Integrated Three-Dimensional Hydrodynamic and Water Quality Model System for Estuarine and Coastal Applications. Marine Technology Society Journal 33 (3): 38-54.

Swanson, J. C., and Ward, M., 2000. Improving Coastal Model Prediction through Data Assimilation. Proceedings of the 6th International Conference on Estuarine and Coastal Modeling, November 3-5, 1999, New Orleans, 10-11.

Wang, P. F., Cheng, R. T., Richter, K., Gross, E. S., Sutton, D., and Gartner, J. W., 1998. Modeling Tidal Hydrodynamics of San Diego Bay, California. Journal of the American Water Resources Association 34 (5): 1123-1140.

Woodward-Clyde, 1996. 1995-1996 City of San Diego and Co-Permittee NPDES Stormwater Monitoring Program Report.

Youssef, M. and Spaulding, M. L., 1993. Drift Current Under the Action of Wind and Waves. Proceedings of the 16th Arctic and Marine Oil Spill Program Technical Seminar, Calgary, Alberta, Canada, pp. 587-615.